MODE DETECTION IN VEHICLES USING A SLIDING MODE ESTIMATOR

Christopher Edwards * **Roderick G. Hebden** *
Sarah K. Spurgeon *

* *Control and Instrumentation Research Group, Department of Engineering, University of Leicester, University Road, Leicester LE1 7RH, U.K.*

Abstract: This paper explores the use of sliding mode observers to detect the onset of potentially dangerous vehicle modes such as oversteer, understeer or split-mu braking. Provided these modes can be detected quickly enough, existing stability controllers can be engaged to ensure safe performance of the vehicle. It is shown that the equivalent output error injection signals associated with the sliding mode observer have distinctive signatures depending on the particular mode which is encountered. Appropriate thresholds on these signals can be set so the scheme ignores variations which arise during the course of normal driving, but can detect and isolate different undesirable vehicle modes within 0.3 seconds of their onset.

Keywords: sliding modes, automotive

1. INTRODUCTION

This paper describes a scheme capable of detecting when a vehicle performing a transient manoeuvre enters a potentially dangerous mode, such as oversteer, understeer, or split-μ braking, to distinguish between these modes, and to give some indication of the severity. This information could then be used, in real-time, to select a control strategy appropriate to the vehicle's circumstances, such as controllers which attempt to improve ride comfort in normal driving, vehicle stability controllers which manipulate individual wheel torques to prevent a vehicle from understeering or oversteering dangerously, or controllers to facilitate safe braking on harsh split-μ surfaces. Various commercial systems now in the marketplace such as Dynamic Stability Control (DSC - BMW, Jaguar); Electronic Stabilization Programme (ESP - Audi, Mercedes-Benz, SAAB) (Bauer, 1999) use a combination of wheel speeds, ABS information, yaw rate, lateral acceleration and steer angle and seek to robustly estimate *all the vehicle states*. In this paper a simpler approach will be adopted which does not attempt to explicitly estimate the states and instead looks for 'signature differences' between the behaviour of an ideal linear vehicle model and the actual measured behaviour. The approach described in this paper makes the assumption that as a vehicle starts to understeer, oversteer, or enters a harsh split-μ braking manoeuvre, *unexpected vehicle yaw moments* and *unexpected lateral forces* will arise. For each of the scenarios, these two signals can reasonably be expected to display differing characteristic signatures. These quantities are difficult to measure directly and instrumentation to do so is unlikely to be fitted to commercial vehicles. Therefore, ideally, any scheme should be

[1] The authors would like to express their thanks to Dr Jim Farrelly from TRW Automotive for his help with this work and EPSRC for their financial assistance.

designed to reconstruct these 'unexpected' signals from more easily measured quantities. In the proposed scheme, it is assumed that measurements of yaw rate, r, and lateral acceleration, a_y, are available. It is also assumed that the front road-wheel steer angle, δ_f and its derivative, are known. The scheme is based on a sliding mode observer, which, using the principle of equivalent output error injection (the natural analogue of the so-called 'equivalent control' (Utkin, 1992)), generates two signals which possess different characteristic signatures depending on the mode in which the vehicle is operating.

2. MODELLING AND OBSERVER DESIGN

The performance of the mode detection scheme will be tested on a nonlinear vehicle model. An 8th order nonlinear model of the vehicle, wheels and road/tyre interaction has been developed, similar to Yu and Moskwa (1994). This model is representative of a typical family saloon – details of the model are given in (Hebden *et al.*, 2004).

A sliding mode observer (Drakunov and Utkin, 1995; Edwards and Spurgeon, 1998) designed around a variation of the so-called bicycle model (MacAdam, 1981) will be used as the basis for the mode detection system. Usually, this model is given in terms of the yaw rate r and side-slip angle. Here, however, it will be given in terms of r and the lateral velocity v to tie in with the nonlinear 8th order model in (Hebden *et al.*, 2004). A schematic of the bicycle model is shown in Figure 1. The equations of motion are derived to include, explicitly, the 'unexpected' moment and force signals, M_{un} and F_{un}.

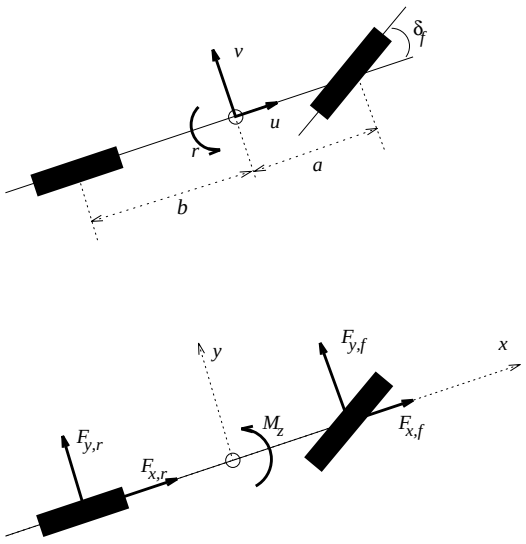

Fig. 1. Bicycle model

From Newtonian mechanics

$$\begin{aligned} I_z\dot{r} &= M_{zf} - M_{zr} + M_{un} \\ &= -2aC_{\alpha f}\alpha_f + 2bC_{\alpha r}\alpha_r + M_{un} \end{aligned} \tag{1}$$

where $C_{\alpha f}$, $C_{\alpha r}$ represent front and rear lateral tyre stiffnesses, and α_f, α_r represent tyre slip-angles at the front and rear of the vehicle respectively and I_z is the inertia. Given that

$$\alpha_f = \frac{v + ar}{u} - \delta_f \tag{2}$$

$$\alpha_r = \frac{v - br}{u} \tag{3}$$

where u and v are the longitudinal and lateral velocities respectively and the coefficients a and b are given in Figure 1, it follows that

$$\dot{r} = \underbrace{\frac{2(bC_{\alpha r} - aC_{\alpha f})}{I_z u}}_{A_{12}} v - \underbrace{\frac{2(a^2C_{\alpha r} + b^2C_{\alpha f})}{I_z u}}_{A_{11}} r + \underbrace{\frac{2aC_{\alpha f}}{I_z}}_{B_1}\delta_f + \frac{M_{un}}{I_z} \tag{4}$$

Given the lateral acceleration $a_y = \dot{v} + ur$ and

$$M_T a_y = F_{yf} + F_{yr} + F_{un} \tag{5}$$

where M_T represents the total mass of the vehicle, it follows that

$$M_T(\dot{v} + ur) = -2C_{\alpha f}\alpha_f - 2C_{\alpha r}\alpha_r + F_{un} \tag{6}$$

and so

$$\dot{v} = \underbrace{-\frac{2(C_{\alpha f} + C_{\alpha r})}{M_T u}}_{A_{22}} v + \underbrace{(\frac{2(bC_{\alpha r} - aC_{\alpha f})}{M_T u}}_{A_{21}} - u)r + \underbrace{\frac{2C_{\alpha f}}{M_T}}_{B_2}\delta_f + \frac{F_{un}}{M_T} \tag{7}$$

For design purposes, the measured outputs are considered to be r and a_y, where

$$a_y = A_{21}r + A_{22}v + B_2\delta_f + \frac{F_{un}}{M_T} \tag{8}$$

For the development which follows, it is convenient to establish new equations in terms of r and a_y. By re-arranging equation (7) and substituting for $\dot{v}$ from the expression for lateral acceleration

$$v = \frac{1}{A_{22}}\left(-(A_{21} + u)r + a_y - B_2\delta_f - \frac{F_{un}}{M_T}\right) \tag{9}$$

Substituting from (9) into equation (4) gives

$$\begin{aligned} \dot{r} = &\left(A_{11} - \frac{A_{12}}{A_{22}}(A_{21} + u)\right) r + \frac{A_{12}}{A_{22}}a_y \\ &+(B_1 - \frac{A_{12}}{A_{22}}B_2)\delta_f + \frac{M_{un}}{I_z} - \frac{A_{12}}{A_{22}}\frac{F_{un}}{M_T} \end{aligned} \tag{10}$$

Differentiating equation (8) and substituting from equation (4) and the expression for a_y yields

$$\dot{a}_y = \left(A_{11}A_{21} - A_{22}u - \frac{A_{12}}{A_{22}}A_{21}(A_{21}+u)\right) r + \left(A_{22} + \frac{A_{12}}{A_{22}}A_{21}\right) a_y + A_{21}(B_1 - \frac{A_{12}}{A_{22}}B_2)\delta_f + B_2\dot{\delta}_f + A_{21}\frac{M_{un}}{I_z} - \frac{A_{12}}{A_{22}}A_{21}\frac{F_{un}}{M_T} + \frac{\dot{F}_{un}}{M_T} \quad (11)$$

Sliding mode ideas (Utkin, 1992) will now be used to estimate the unknown signals $\dot{F}_{un}$, F_{un}, M_{un}. The estimator uses two discontinuous injection signals, ν_r and ν_a, to force the observed states, $\tilde{r}$ and $\tilde{a}_y$, to track the measured states of the system, r and a_y, from equations (10) and (11), perfectly. Specifically, the estimator takes the form:

$$\dot{\tilde{r}} = \left(A_{11} - \frac{A_{12}}{A_{22}}(A_{21}+u)\right)\tilde{r} + \frac{A_{12}}{A_{22}}\tilde{a}_y + \left(B_1 - \frac{A_{12}}{A_{22}}B_2\right)\delta_f + \nu_r \quad (12)$$

$$\dot{\tilde{a}}_y = \left(A_{11}A_{21} - A_{22}u - \frac{A_{12}}{A_{22}}A_{21}(A_{21}+u)\right)\tilde{r} + \left(A_{22} + \frac{A_{12}}{A_{22}}A_{21}\right)\tilde{a}_y + B_2\dot{\delta}_f + \nu_a + A_{21}\left(B_1 - \frac{A_{12}}{A_{22}}B_2\right)\delta_f \quad (13)$$

where

$$\nu_r = -\rho_r \mathrm{sign} e_r \quad (14)$$

$$\nu_a = -\rho_a \mathrm{sign} e_a \quad (15)$$

and $e_r = \tilde{r} - r$ and $e_a = \tilde{a}_y - a_y$. The positive scalars ρ_r and ρ_a must be chosen large enough to induce a sliding motion on $e_r = 0$ and $e_a = 0$. Once sliding is attained, $\dot{e}_r = \dot{e}_a = e_r = e_a = 0$, and it can be shown from (10)-(13) that

$$0 = \bar{\nu}_r - \frac{M_{un}}{I_z} + \frac{A_{12}}{A_{22}}\frac{F_{un}}{M_T} \quad (16)$$

$$0 = \bar{\nu}_a - A_{21}\frac{M_{un}}{I_z} + A_{21}\frac{A_{12}}{A_{22}}\frac{F_{un}}{M_T} + \frac{\dot{F}_{un}}{M_T} \quad (17)$$

where $\bar{\nu}_r$ and $\bar{\nu}_a$ are the equivalent output error injection signals necessary to maintain sliding (Utkin, 1992) in the face of F_{un} and M_{un}. Information about the unexpected signals can be obtained from (16)-(17) using the injection signals. Note that a component of the second injection signal, $\bar{\nu}_a$, is a scaling of the first injection signal, $\bar{\nu}_r$, and that, by subtracting this component, $\bar{\nu}_a$ can be used to obtain an estimate of the unexpected signal, $\dot{F}_{un}$. The first injection signal, $\bar{\nu}_r$, provides a weighted average of the unexpected signals, M_{un} and F_{un}. As M_{un} and F_{un} are free to vary independently, this injection signal alone cannot be used to determine them explicitly without further information. From the parameter values in (Hebden *et al.*, 2004), it can be shown that $\bar{\nu}_r$ is dominated by the unexpected yaw moment, M_{un} since $\frac{A_{12}}{A_{22}} = 0.2026$ (and is independent of forward speed u).

3. MANOEUVRE DETECTION

In this section, the various manoeuvres will be discussed in turn, each with a hypothesis outlining the characteristic signatures which might be expected. By definition, the unexpected signals occur whenever the system deviates from ideal linear behaviour, and so can be considered as the nonlinear component of the total yaw moment and lateral force signals. In the non-linear model from (Hebden *et al.*, 2004) it is possible to extract the (total) values for the vehicle yaw moment and lateral force, and to differentiate the latter (within the Simulink model) to give $\dot{F}_y$. The linear, 'expected' signals $M_{zl} = M_{zf} - M_{zr}$ and $F_{yl} = F_{yf} + F_{yr}$ can be calculated from the linear components of equation (1) and equation (5) using the values of u, v and r from the nonlinear simulation to calculate tyre slip from (2)-(3). The linear expected signals can be subtracted to obtain the 'unexpected' signals. These can be compared with the reconstructions from the sliding mode estimator to assess its accuracy.

In an *understeer manoeuvre*, the actual yaw rate experienced by the vehicle is less than the yaw rate which would be expected if the vehicle were operating linearly. For this reason, it is reasonable to assume that the build up of understeer would be accompanied by an 'unexpected' yaw moment, M_{un}, in a direction away from the turn. The front tyres will saturate leading to an increase in front wheel slip-angles and increased lateral force, away from the turn, at the front of the vehicle. In a left turn (as in the simulation), $F_{yf} > 0$, $F_{yr} > 0$, $F_{y,l} > 0$ and $M_{z,l} > 0$ and the unexpected force and yaw moments $F_{un} < 0$ and $M_{un} < 0$.

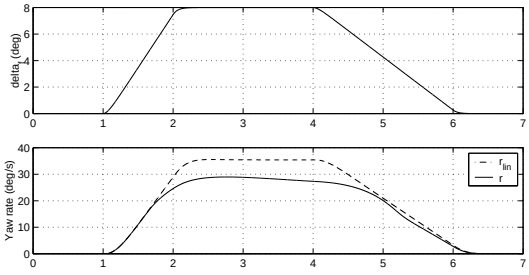

Fig. 2. Understeer manoeuvre

Figure 2 shows an understeer manoeuvre performed on the nonlinear simulation described in (Hebden *et al.*, 2004). The first plot shows the road-wheel steering angle and results in a left turn. The second plot compares the actual yaw rate from the nonlinear model with the expected yaw rate, taken from a linear model.

In an *oversteer manoeuvre*, the actual yaw rate experienced by the vehicle is greater than the yaw rate which would be expected if the vehicle were operating linearly. For this reason, it is expected that the build up of oversteer would be accompanied by an additional 'unexpected' yaw moment, M_{un}, in the same direction as the turn. The rear tyres will saturate leading to an increase in rear wheel slip-angles and increased lateral force, away from the turn, at the rear of the vehicle. In a left turn $F_{yf} > 0$, $F_{yr} > 0$, $F_{y,l} > 0$ and $M_{z,l} > 0$ and so the unexpected signals should have the characteristics $F_{un} < 0$ and $M_{un} > 0$.

A dynamic oversteer manoeuvre usually consists of a series of oversteer regions, each one greater than the last. The reconstruction signals in each oversteer region should be progressively greater in magnitude and should alternate in direction. In order to encourage the vehicle in the simulation to oversteer, the coefficient of friction on the two rear tyres has been dropped (artificially) from 0.8 to 0.5. This has the effect of reducing the traction available to the rear tyres.

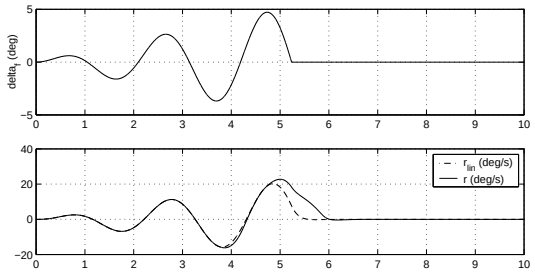

Fig. 3. Dynamic oversteer manoeuvre

Figure 3 shows the dynamic oversteer manoeuvre. The first plot shows the road-wheel steering angle. The second plot compares the actual yaw rate of the nonlinear model with the expected yaw rate, taken from a linear model. As a region of oversteer is entered, the actual yaw-rate begins to exceed the expected yaw-rate of the linear model. Two oversteer manoeuvres are seen, one at around 3.75 sec, and also at around 4.75 sec.

Finally, the nonlinear vehicle model simulates a harsh *split-μ braking* manoeuvre on a surface where the friction coefficient for the wheels on the passenger side differ from those on the driver's side. In this case, the values $\mu = 0.8$ and $\mu = 0.2$ have been used. Throughout the simulation, the steering angle has been kept at zero. Here, an emergency stop situation is simulated whereby a simple model of an ABS system brings the vehicle to a stop as soon as possible. The front high-μ wheel reaches its peak braking torque at ≈ 0.5 secs. At 0.7s, the vehicle leaves the split-μ surface and enters a homogeneous surface with $\mu = 0.8$. The simulation runs open-loop and the vehicle is allowed to drift toward the high-μ surface.

In this scenario, it is expected that there would be an initial unexpected yaw moment – due to the asymmetric braking – with any unexpected lateral force building up more slowly, as a result of the assumed yaw angle. As the braking torque reaches a peak, the unexpected yaw moment should level off, leaving the lateral force continuing to build up. As the vehicle leaves the split-μ surface, the unexpected yaw moment should rapidly decrease as traction returns to the tyres and the braking becomes symmetrical.

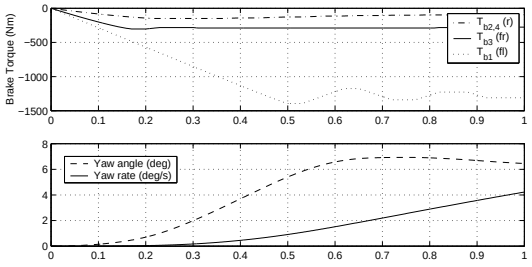

Fig. 4. Split-μ braking manoeuvre

Figure 4 shows the split-μ braking manoeuvre on the nonlinear vehicle simulation. The first plot shows the four brake torques (T_{b1} - front left, T_{b2} - rear left, T_{b3} - front right, T_{b4} - rear right). The two rear brake torques coincide on the plot due to the 'select-low' strategy (Bauer, 1996).

Based on these observation characteristic signatures associated with $\dot{F}_{un}$ and $\bar{\nu}$ are:

- An *understeer* manoeuvre may be detected by a sudden increase in both the reconstruction signals *in the same direction*. As the severity of the understeer manoeuvre reaches a peak value, the $\bar{\nu}_r$ signal should level off, and the $\dot{F}_{un}$ signal decrease and switch sign.
- An *oversteer* manoeuvre may be detected by a sudden increase in the reconstruction signals *in opposite directions*. As the severity of the oversteer manoeuvre reaches a peak value, the $\bar{\nu}_r$ signal should level off, and the $\dot{F}_{un}$ signal decrease and switch sign.
- A harsh *split-μ braking* manoeuvre may be detected by the presence of a sudden ramping of the $\bar{\nu}_r$ reconstruction signal with no initial accompanying increase in the $\dot{F}_{un}$ signal.

4. VEHICLE MODE PREDICTION

The key observation from the previous section is that the unexpected signals which are reconstructed vary significantly between the manoeuvres. However, for a mode detection scheme to be useful, it must be able to predict the onset of a severe mode before it poses a risk, so that preemptive action may be taken.

The method proposed for predicting the various modes requires the definition of appropriate

thresholds for the two reconstruction signals. Here values of ± 0.25 and ± 1000 have been chosen for $\bar{\nu}_r$ and $\dot{F}_{un}$ respectively. It can be verified that in the earlier simulations, during any of the modes, these thresholds would be crossed.

Noise with a standard deviation approximately 5% of the measurement range was added to both output signals in the simulation. In the proposed prediction scheme the undesirable effects of the noise have been minimized by selecting the scalar gains of the sliding mode estimator from (15) and (14) as $\rho_r = \rho_a = 10$ and applying a low pass filter to the reconstruction signals exiting the observer. This is still in keeping with the notion of the equivalent injection signals $\bar{\nu}_r$ and $\bar{\nu}_a$ as the low frequency components of the switching terms ν_a and ν_r (Utkin, 1992). However, whilst this filter attenuates the noise, it also produces a time-delay in the reconstructed signal. A satisfactory trade-off between the requirements for noise reduction without a significant reconstruction signal time-delay has been found using a first order filter with time constant 1/10.

4.1 A detection algorithm

The algorithm chosen to identify the vehicle mode is based on the variables t_1, t_2 and $\Delta t = t_2 - t_1$:

(1) When either reconstruction signal crosses a threshold, define t_1 to be the time when the threshold is crossed. Isolate whether $\dot{F}_{un}$ or $\bar{\nu}_r$ has triggered the alarm and which side of the threshold has been crossed. For both signals at time t_1 record a reading of '0' (within thresholds), '+' (if the +ve threshold is violated) or '−'(if the −ve threshold is violated).

(2) Continue to monitor the two detection signals. If the other detection signal crosses a threshold, set t_2 to be the time at which the threshold is crossed and compute $\Delta t = t_2 - t_1$ i.e. the length of time necessary to make the prediction. Otherwise, if the original detection signal drops below its threshold without the second signal crossing a threshold, reset the algorithm.

Figures 5-8 show a few seconds of each simulation around the point at which the vehicle begins a manoeuvre. For example, Figure 5 shows the reconstruction signals around the point at which the vehicle first enters the understeer region of the simulation. These plots are taken from the same simulations presented earlier. The solid line is the actual $\dot{F}_y$ signal; and the 'dashed' line corresponds to the reconstructed signal after filtering.

The results of the simulations are summarized in Table 1. The quantity Δt, in Table 1, represents the time between the first filtered reconstruction signal crossing a threshold and the point at which a prediction can be made. The detection time in each case requires approximately an additional 0.08 secs to be added to the values in Table 1 because of the lag associated with the filter.

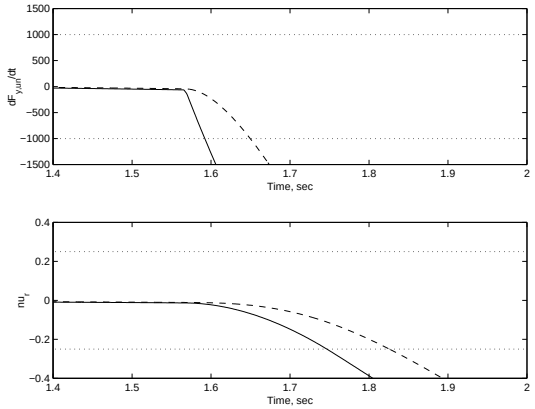

Fig. 5. Prediction: Understeer

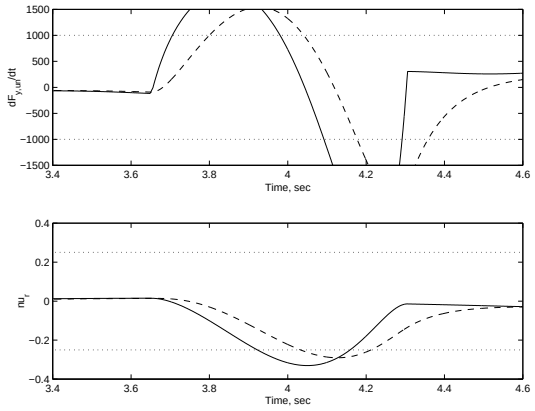

Fig. 6. Prediction: Dynamic Oversteer - Region 1

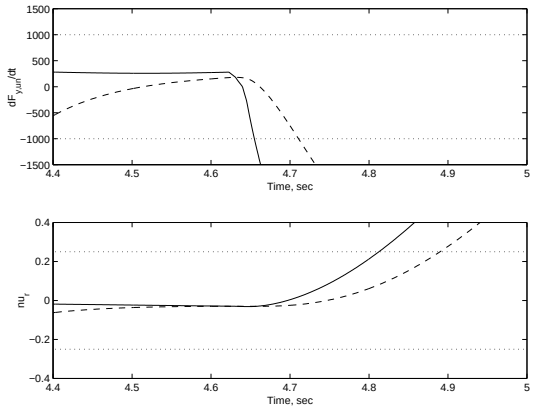

Fig. 7. Prediction: Dynamic Oversteer - Region 2

	1^{st} **Reading**			2^{nd} **Reading**			
Scenario	$t_1(s)$	$\dot{F}_y$	ν_r	t_2 (s)	$\dot{F}_y$	ν_r	$\Delta t(s)$
Understeer	1.65	−	0	1.85	−	−	0.20
Oversteer 1	3.80	+	0	4.02	+	−	0.22
Oversteer 2	4.71	−	0	4.91	−	+	0.20
Split-μ	0.30	0	+	0.52	−	+	0.22

Table 1. Prediction Readings

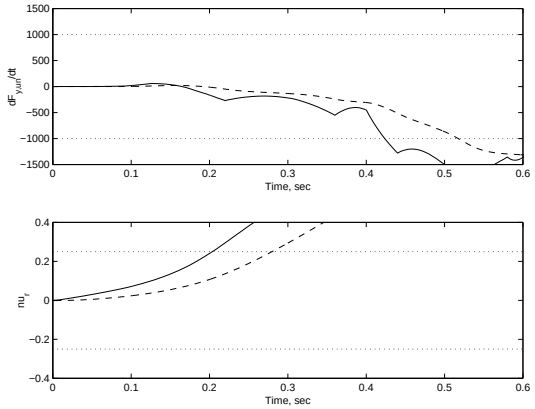

Fig. 8. Prediction: Split-μ Braking

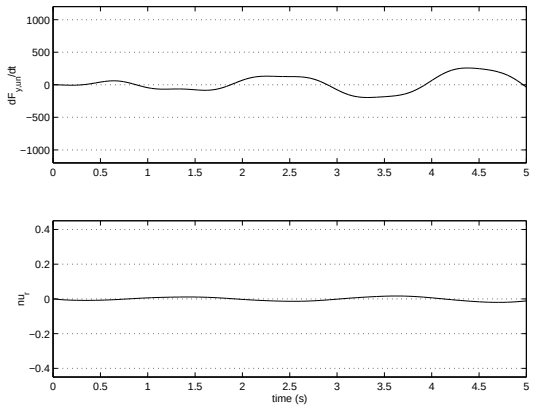

Fig. 9. Prediction: Chicane

In the case of understeer (Figure 5), it can be seen that the first signal to cross its threshold is the $\dot{F}_y$ signal. At this point the algorithm defines $t_1 = 1.65s$, and would rule out a split-μ braking manoeuvre as the $\dot{F}_y$ signal is crossed first. The $\bar{\nu}_r$ signal then crosses its threshold giving $t_2 = 1.85s$ and $\Delta t = 0.2s$. At this point the algorithm would deduce that a severe understeer manoeuvre is likely as both the signal thresholds crossed had the same sign. This information could then be communicated to an overall monitoring scheme and the appropriate controller could be engaged.

The $\dot{F}_y$ signal is first to cross its threshold for each of the oversteer manoeuvres (Figures 6-7), which suggests that either severe understeer or oversteer is likely. In each case the $\bar{\nu}_r$ signal then crosses its threshold, and in each case the two thresholds crossed have opposite signs, which implies an impending severe oversteer manoeuvre.

The split-μ braking manoeuvre (Figure 8) stands out from those studied as it is the only manoeuvre in which the $\bar{\nu}_r$ signal crosses its threshold first.

All these timings depend on the choice of threshold. In order to determine that a suitable choice has been made a severe 'chicane' manoeuvre which involves significant lateral dynamics whilst avoiding significant under/oversteer, has been considered. This involves the δ_f signal following a sinusoid of amplitude 3° at a frequency of 3 rad/sec. The unexpected signals associated with this manoeuvre are shown in Figure 9 and are well within the set thresholds. (A more realistic lane change manoeuvre has also been considered in which the vehicle undergoes a lateral shift of 3.65m in 4 secs. This is less severe and produces unexpected signals which are visually zero.) Therefore normal driving is not likely to provoke a false alarm.

5. CONCLUSIONS

Using sliding mode observer concepts, a vehicle mode detector and predictor has been presented. The mode prediction is based upon reconstructing certain signals which would be unexpected in a vehicle behaving in a linear fashion, and identifying distinctive signatures in these signals in the early stages of the build-up to a severe vehicle mode. The method utilizes an algorithm which allows the scheme to not only detect a severe manoeuvre, but also to predict likely severe manoeuvres before they become dangerous. Appropriate thresholds have been chosen such that the scheme ignores signal variations which may arise in the course of normal driving.

REFERENCES

Bauer, H. (1996). *Automotive Handbook, 4^{th} Edition*. Robert Bosch GmgH, Stuttgart (Translation editor in chief: Peter Girling) Distributed by SAE Society of Automotive Engineers, PA, USA.

Bauer, H. (1999). *ESP Electronic Stability Program*. Robert Bosch GmgH, Stuttgart.

Drakunov, S. and V.I. Utkin (1995). Sliding mode observers: tutorial. In: *Proceedings of the 34th IEEE Conference of Decision and Control*. pp. 3376–3378.

Edwards, C. and S.K. Spurgeon (1998). *Sliding Mode Control: Theory and Applications*. Taylor & Francis.

Hebden, R.G., C. Edwards and S.K. Spurgeon (2004). Automotive stability in a split-mu manoeuvre using an observer based sliding mode controller. *International Journal of Vehicle System Dynamics* **41**, 181–203.

MacAdam, C. (1981). Application of an optimal preview control for simulation of closed-loop automobile driving. *IEEE Transactions on Systems, Manufacturing and Cybernetics* **SMC-11**(6), 393–399.

Utkin, V.I. (1992). *Sliding Modes in Control Optimization*. Springer-Verlag, Berlin.

Yu, S.H. and J.J. Moskwa (1994). A global approach to vehicle control: Coordination of four wheel steering and wheel torques. *ASME Journal of Dynamic Systems Measurement and Control* **116**, 659–667.